

Article

Transition of Sulphide Self-Heating from Stage A to Stage B †

Sungjae Moon, Frank Rosenblum, Yuehua Tan, Kristian E. Waters  and James A. Finch *

Department of Mining and Materials Engineering, McGill University, 3610 University Street, Montreal, QC H3A 0C5, Canada; sungjae.moon@mail.mcgill.ca (S.M.); frank.rosenblum@mcgill.ca (F.R.); yue.tan@mcgill.ca (Y.T.); kristian.waters@mcgill.ca (K.E.W.)

* Correspondence: jim.finch@mcgill.ca; Tel.: +1-514-398-1452

† This is an extended paper from International Mineral Processing Congress (IMPC) XXX.

Received: 18 October 2020; Accepted: 10 December 2020; Published: 17 December 2020



Abstract: Previous work has shown that sulphide self-heating occurs in three distinct stages, referred to as Stage A, Stage B and Stage C. In this publication, the focus is the transition from Stage A to Stage B which occurs at ca. 100 °C. Background literature hints that the transition corresponds to the transformation of the rhombic form of elemental sulphur to the more reactive monoclinic form that occurs at 96 °C. A test apparatus is modified for adiabatic heating to track the transition. The results support this transformation of sulphur as being key to the transition, and the transition temperature is thus modified to 96 °C. Variations in a sample's response under adiabatic conditions are observed and possible reasons are discussed. Testing in adiabatic mode provides new insights into the sulphide self-heating process that complements the test designed to identify propensity to self-heat.

Keywords: self-heating; stage A/stage B; transition; rhombic/monoclinic elemental sulphur; adiabatic heating

1. Introduction

Some materials, when exposed to ambient conditions, can exhibit a rise in temperature without requiring an external heat source. Generally referred to as pyrophoric or self-heating substances, they pose a challenge to the safe handling of materials in storage and transportation. Numerous substances self-heat, ranging from wood chips and powdered milk to coal and sulphide minerals [1,2]. Combinations of sulphide minerals, most notably those containing the iron sulphide pyrrhotite ($\text{Fe}_{(1-x)}\text{S}$), commonly encountered in the extraction of base metals (e.g., copper, zinc, lead, and nickel), are particularly prone to self-heating [3,4]. If not controlled, sulphide self-heating can lead to work disruptions, loss of infrastructure, delays in operations and in some severe cases, loss of life [5]. Dramatic examples include in-situ smelting of ores and resultant fires [5,6] and loss of a ship transporting Cu-concentrate [7].

Testing for sulphide self-heating risk is required by the International Maritime Solid Bulk Cargoes Code [8] and tests continue to be proposed [9–12]. Recent work [13] has shown that the U.N.-recommended test can give false negatives and provides an alternative.

Studies on sulphide self-heating mechanisms identify moisture as key to exothermic reactions with elemental sulphur as one the products [14,15], the critical range being about 3–8% *w/w* [16]. Therein lies a conundrum: as moisture is consumed in the reactions and evaporated as temperature rises to ca. 100 °C, what causes the further temperature rise? Rosenblum and co-workers [3,17–20] have argued that sulphide self-heating follows a three stage process: Stage A, up to ca. 100 °C, where moisture is present and elemental sulphur is produced; Stage B, ca. 100 °C to 350 °C, where the sulphur oxidizes; and Stage C, above ca. 350 °C, when direct oxidation of the sulphides occurs

(i.e., smelting). Studies have largely concentrated on the properties of the individual stages, with no studies reported on the transitions between the stages. Without transition from Stage A to Stage B, for example, the runaway condition Stage C, which causes most of the problems, does not occur.

The present paper focuses on the factors associated with the Stage A to Stage B transition. We start with a review of the literature related to the transition.

2. A Brief Review of Self-Heating Literature Related to the Transition

In Rosenblum and Spira [18] the notional temperatures at which the transitions occurred were identified. The paper also described the test apparatus and protocol designed to assess Stages A and B (now referred to as the FR-2 apparatus and test). Stage A (i.e., below ca. 100 °C) conditioning (or “weathering”) was simulated using a thermally active waste rock sample from Brunswick Mining and Smelting. The sample was dry ground then moistened to 8% moisture. The sample was subjected to cycles of 15 min air injection every 5 h. Weathering at 50 °C showed that elemental sulphur was generated (Figure 1) along with other oxidation products (in this example, goethite and sulphates) and that the pyrrhotite, which was the source of the oxidation products, diminished with weathering time.

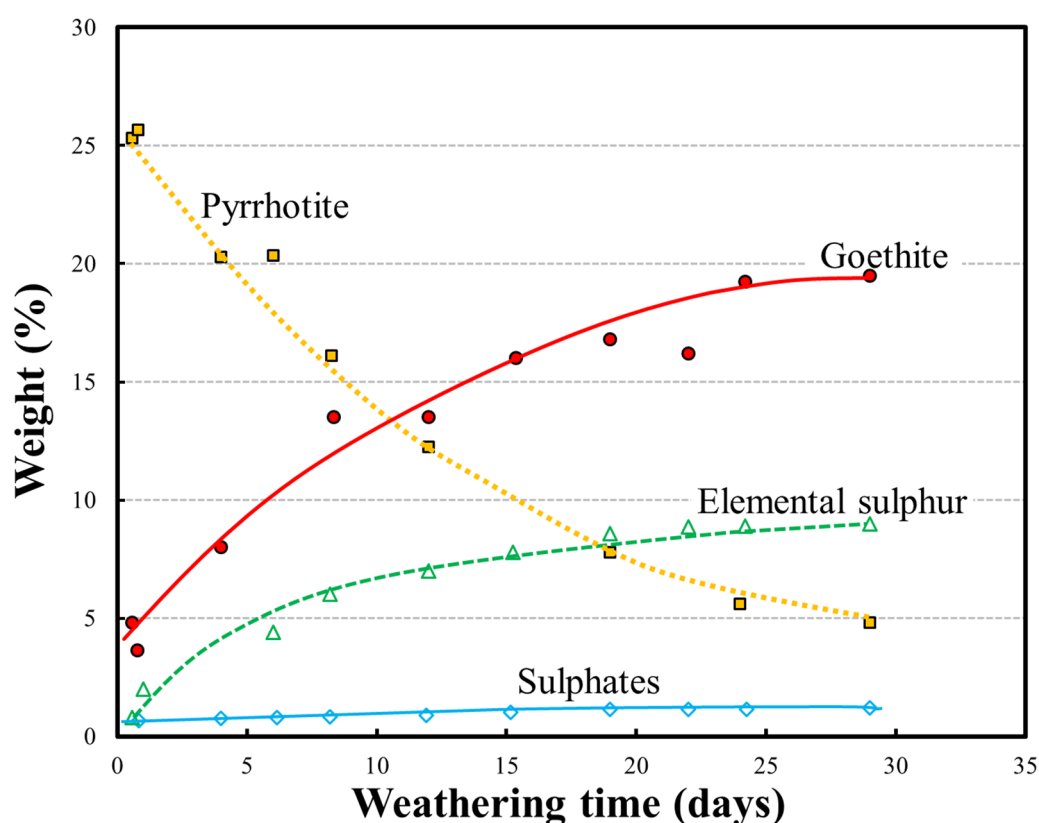


Figure 1. Effect of weathering in Stage A at 50 °C on reduction in pyrrhotite content and increase in oxidation products (adapted from Rosenblum and Spira [18]).

Using differential scanning calorimetry (DSC), the heat-generating potential of a sulphide ore sample was assessed (Figure 2). The fresh (un-weathered) sample exhibited practically zero heating and with increased weathering (at 40 °C) the exothermic peaks increased showing a direct correlation between the extent of weathering and heat generation. In terms of the stages, the weathering was in Stage A with resultant heat flow occurring in Stage B (DSC peaks are >100 °C).

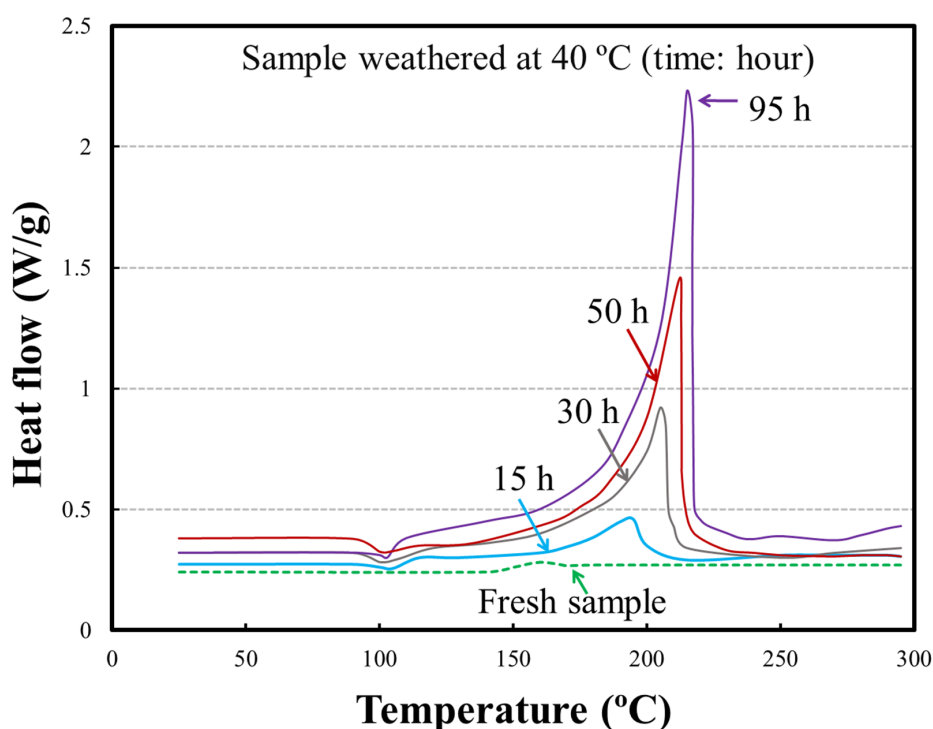


Figure 2. Effect of weathering in Stage A at 40 °C on DSC exotherms (adapted from Rosenblum and Spira [18]).

In an extension to the results in Figure 2, which represents about 4 days, weathering was conducted at 50 °C for 45 days followed by DSC measurements (Figure 3). The heat flow continued to increase with increased weathering, reaching a maximum at about 20 days then dropping, reaching a plateau, followed by a further drop. Based on the prior results, the following was argued to be the sequence of events giving rise to these swings in reactivity. In the initial stage of weathering elemental sulphur is formed which becomes the fuel that drives the observed exothermic reaction in the DSC test (i.e., Stage B reaction/s). With increased weathering, the other oxidation products (oxides, etc.) that are formed could interfere with the oxidation of the elemental sulphur thus reducing the heat flow. Note that after washing, filtering and drying the 45-day weathered sample, reactivity increased significantly. A suggestion is that washing either dissolved or dislodged the oxides, etc., which are also formed, thus exposing more of the elemental sulphur resulting in increased heating.

In the 1995 publication [9] SO₂ off-gas was measured as a function of temperature. Figure 4 (open symbols, % scale) shows SO₂ began to appear at about 100 °C and with increasing temperature substantially more SO₂ was generated. From these results, it appears that SO₂ is emitted in Stage B only.

Included in the figure is experience at one mine site [21] where high levels of SO₂ were detected which prompted measurements to correlate SO₂ emissions with the corresponding in situ temperature. Results (closed symbols, ppm scale) showed that most data fell above 100 °C, that is, corresponding to a Stage B event. When plotting sulphur vapour pressure as a function of temperature [22], it is noted that vapour first appears at a temperature above ca. 100 °C (dashed curve).

These results support the interpretation that self-heating of sulphides proceeds in at least two distinct stages: Stage A, where the presence of moisture causes exothermic reactions producing elemental sulphur, followed by Stage B, where the sulphur oxidizes to generate heat and sulphur dioxide. There is evidence [23] that the elemental sulphur formed in Stage A is the rhombic form (α -S8) which is stable below 96.5 °C, and above this temperature it transitions to the less stable monoclinic form (β -S8) that readily oxidizes to generate heat and SO₂. As an average we adopt a sulphur-form transition temperature of 96 °C, the range being from 95 °C [23–25] to 96.5 °C [26].

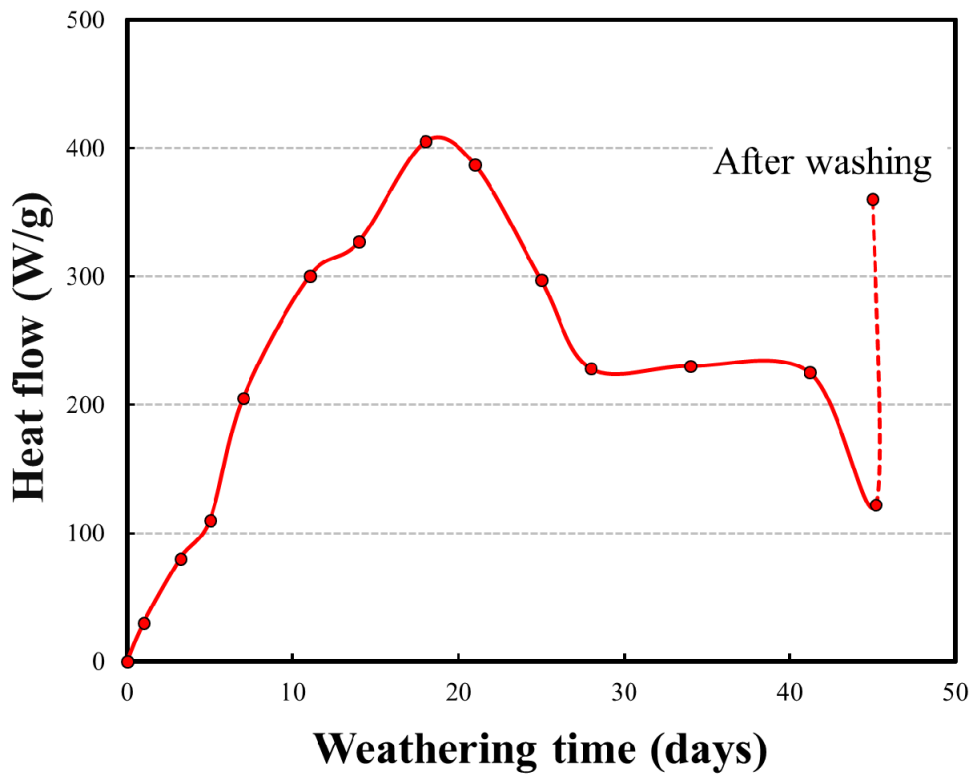


Figure 3. Change in DSC exotherm as a function of extended weathering time (adapted from Rosenblum and Spira [18]).

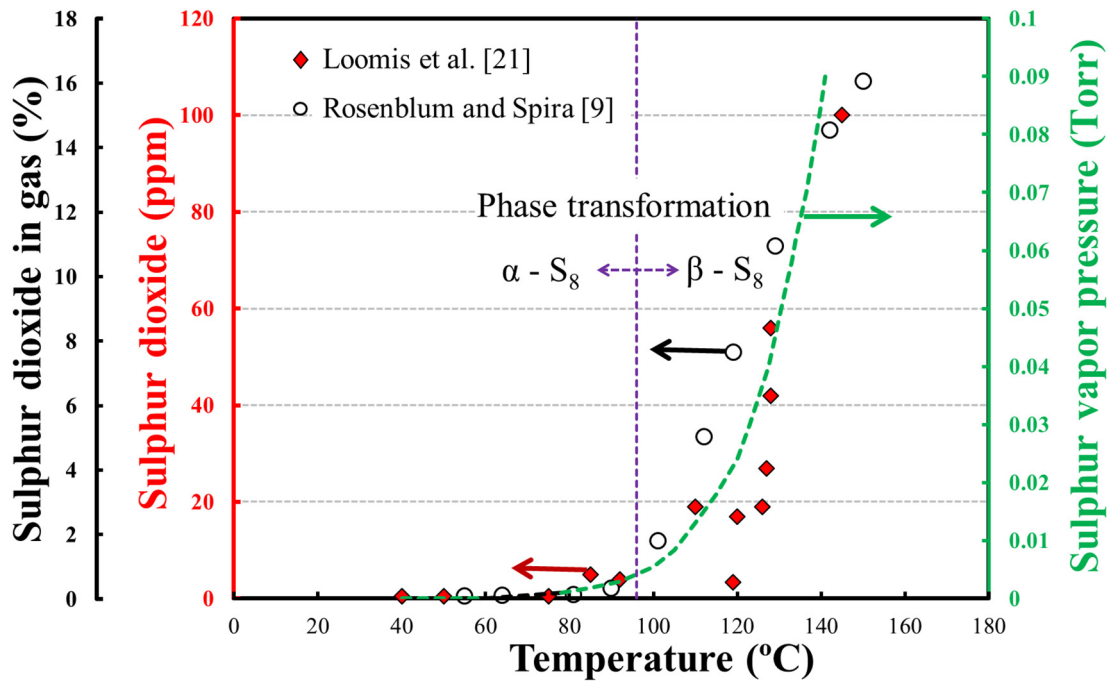


Figure 4. Compilation of literature data as a function of temperature: emission of SO₂ from lab test [9] and mine site [21]; sulphur vapour pressure; phase transition.

With this background, experiments were designed to identify factors affecting the Stage A to Stage B transition.

tested at the standard Stage A condition (70 °C; 10 cycles). Some of these samples were also analyzed for elemental sulphur. There were two objectives: (1) to correlate weathering with the generation of elemental sulphur; and (2) correlate the effect of weathering (number of cycles) with self-heating capacity of Stage A.

3.2.4. Transition Stage A to Stage B

Both the as received and weathered samples were tested. The apparatus was first set to CTC mode (70 °C) with no air injection. After the sample reached the set temperature, control was switched to ATC mode. At that point, air injection (100 mL/min) commenced. To prevent runaway temperatures (that can result in a fire), the ATC mode was limited to 140 °C, at which point it was switched back to CTC mode. When the sample temperature equilibrated with the oven temperature, the oven was shut-off.

3.2.5. Sulphur Determination

On selected samples, elemental sulphur was determined using the carbon disulphide method which brings elemental sulphur directly from the sample into solution [28]. Five-gram samples were contacted with 15 mL carbon disulphide (Sigma-Aldrich, 99.9% A.C.S reagent grade) in a 50 mL beaker, stirred for 10 min then filtered into a 50 mL flask. To ensure that all the sulphur had been recovered, an additional 5 mL carbon disulphide was added, the contents stirred and filtered into the same 50 mL flask. The filtrate was evaporated using an overhead fan in a fume hood and weighed to determine the elemental sulphur content (%).

4. Results

4.1. Weathering

4.1.1. Effect on Elemental Sulphur Generation

Figure 6 shows that increased weathering increased the formation of elemental sulphur. The as-received RMD sample (i.e., zero weathering) had less than 0.1% sulphur, which after 15 cycles rose to 1.8%. In contrast, the as-received Ni Con sample contained almost 1% elemental sulphur (suggestive of prior weathering) and weathering only marginally increased the sulphur content.

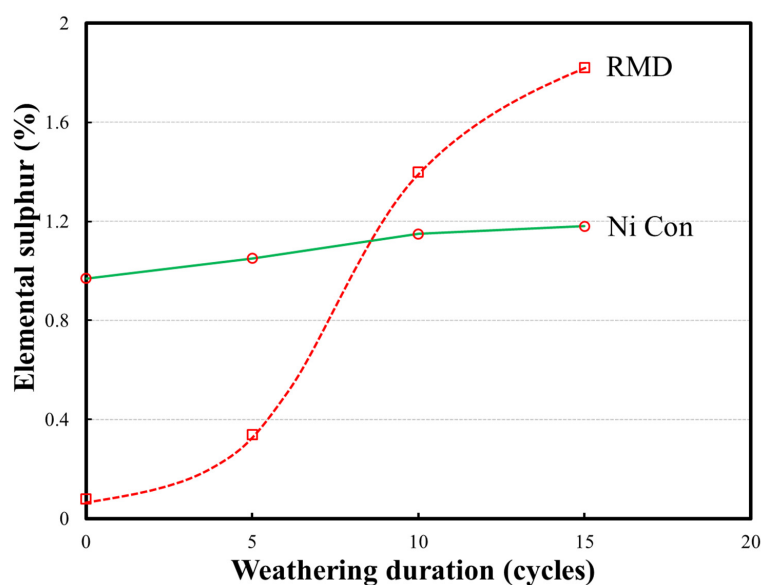


Figure 6. Effect of weathering on the generation of elemental sulphur: RMD and Ni Con samples.

4.1.2. Effect on Self-Heating

Starting at ten weathering cycles, Figure 7 shows that increased weathering cycles resulted in increased Stage A self-heating capacity for both the RMD and Ni Con. The rate of increase for both is similar (lines almost parallel). The higher values exhibited by RMD are attributed to the fact that after the initial 10 weathering cycles there was more elemental sulphur present compared with the Ni Con sample (Figure 6).

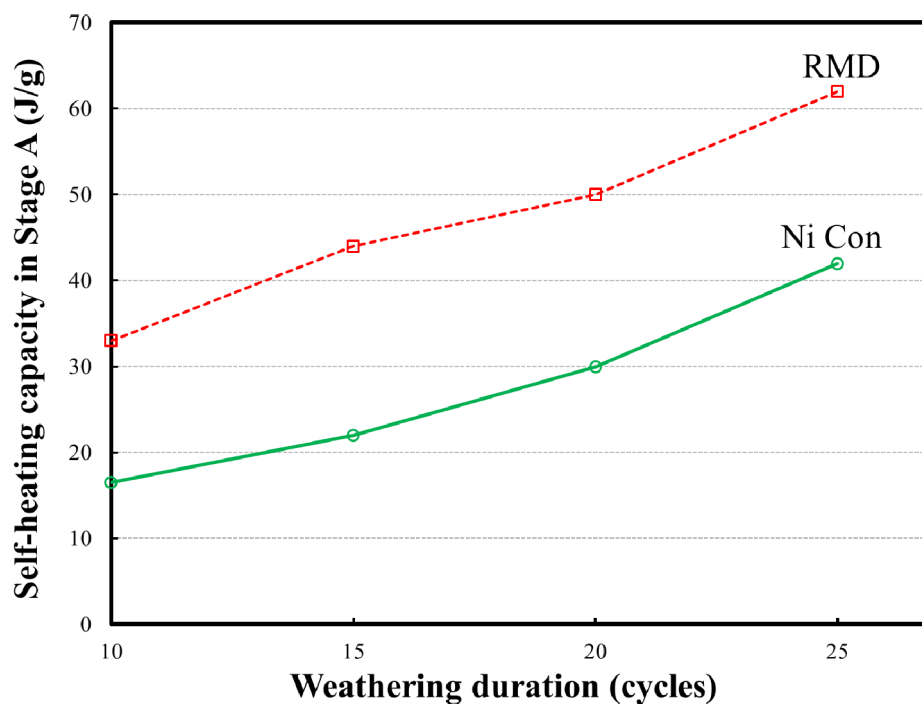


Figure 7. Effect of weathering on Stage A self-heating capacity (for calculation for self-heating capacity see [3]).

4.2. Transition from Stage A to Stage B

4.2.1. Example of a Successful Transition

The sample temperature was first raised to 70 °C under CTC mode with no airflow. When stabilized, control was changed to ATC mode and air injection started (Figure 8). The sample temperature increased, plateaued near the transition temperature for about 3 h (10 h to 13 h) then continued to rise. At 140 °C oven temperature control was changed back to CTC mode, with sample temperature continuing to rise reaching a maximum of 166 °C then dropping back. The temperature rise from 70 °C to ca. 100 °C represents Stage A self-heating while the further temperature rise to 166 °C represents Stage B self-heating. Stage B was sustained for about 8 h (13 h to 21 h) when the sample temperature began to drop, which is consistent with the fuel, elemental sulphur, having been consumed.

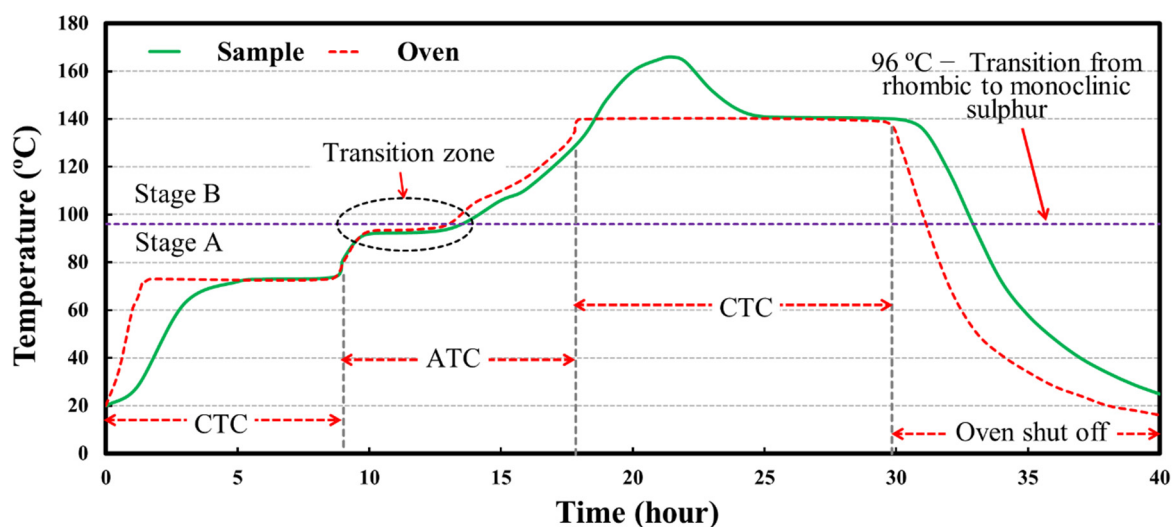


Figure 8. Example thermograph of a sample that passed the transition temperature (shown from initiation to completion of test).

4.2.2. Example of Failure to Transition

In an expanded first part of the temperature response, Figure 9 shows that in this case while the sample temperature rose when the system was switched to ATC mode, it did not pass the transition temperature.

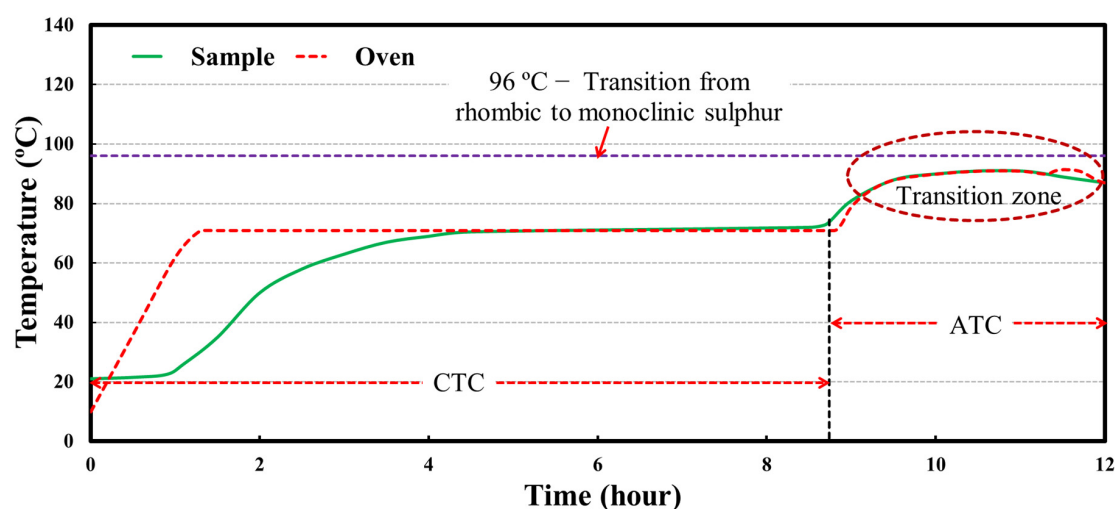


Figure 9. Thermograph of a test sample that did not pass the transition temperature.

4.2.3. Transition and Weathering

The RMD samples weathered for various durations and analyzed for elemental sulphur were remoistened to 6% and then evaluated for the transition from Stage A to Stage B. Using the maximum sample temperature recorded (see Figure 8) to characterize the sample’s self-heating propensity, Figure 10 shows a bell-shaped response: the sample with less than 0.5% sulphur did not pass the transition (in fact did not self-heat as the temperature remained at 70 °C), samples from ca. 0.6% to 1.5% sulphur showed increasing maximum temperatures, and samples with greater than 1.5% sulphur showed a decrease in maximum temperature. The decrease is attributed to the growing presence of other oxidation products (sulphates, oxides/hydroxides), which appear to restrict access of oxygen to the elemental sulphur.

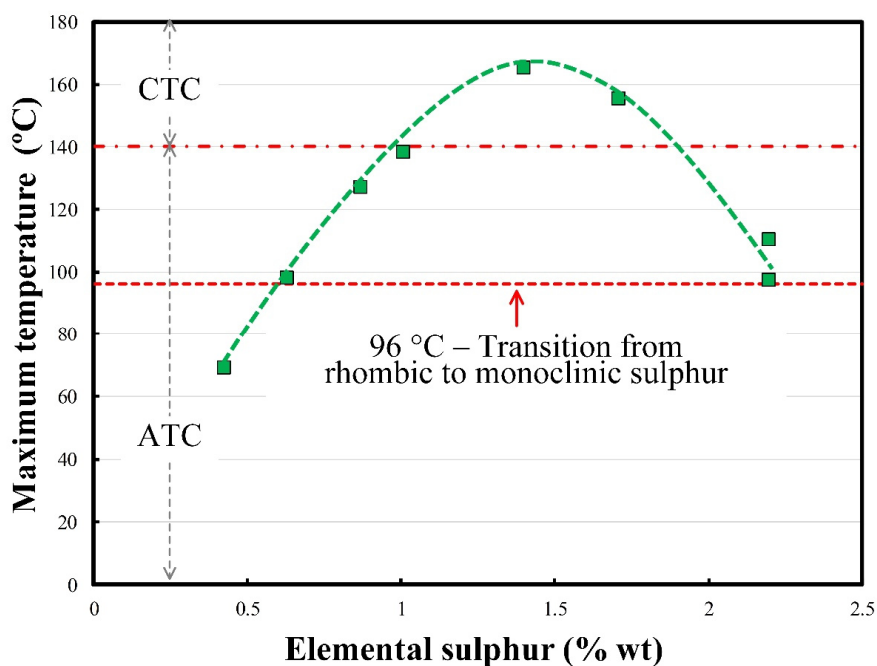


Figure 10. Elemental sulphur and transition from Stage A to Stage B: RMD sample.

A second test series used the Ni Con, which entailed weathering of two samples in duplicate (at 5 and 20 cycles) and one sample in triplicate (at 10 cycles) with testing in ATC mode. Figure 11 shows that for the duplicate at 5 cycles both samples transitioned to Stage B and reached a maximum temperature of ca. 130 °C. The other duplicate (at 20 cycles) and the triplicate sample (10 cycles), however, produced a range of results from just reaching the transition temperature to rising above 140 °C.

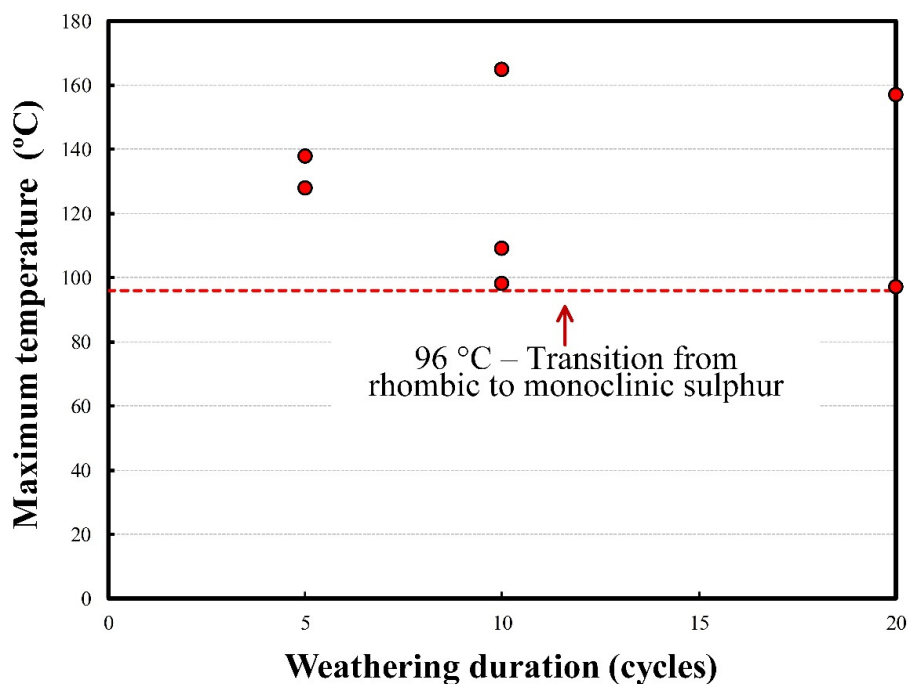


Figure 11. Weathering and transition from Stage A to Stage B: Ni Con sample.

5. Discussion

The original hypothesis was that transition from Stage A to Stage B occurs at 100 °C; that Stage A involved the formation of elemental sulphur which was the fuel for Stage B. Based on the literature and the present findings, the current interpretation refines Stage A as up to 96 °C, corresponding to the transition from rhombic sulphur (α -S8) to the more reactive monoclinic sulphur (β -S8).

In this interpretation, the self-heating in Stage A is the result of exothermic oxidation of sulphides in the presence of moisture that generates rhombic elemental sulphur. Under favorable conditions, the material could reach 96 °C and the sulphur start to transition to the monoclinic form which requires latent heat. Figure 8 appears to show this latent heat, the temperature remaining roughly constant around 96 °C for a period before continuing to rise. This transition time could range from minutes to days and may not always occur.

Failure to pass the transition temperature can have several causes. Some possibilities include: (1), moisture level may decrease below that to sustain Stage A reactions (moisture is consumed in the reactions and is lost to evaporation and replenishment via humidity may not be sufficient); (2), while transition probability increases with sulphur content (i.e., weathering), the increasing level of other oxidation products, sulphates, oxides, etc., may act to coat surfaces and prevent oxygen from reaching the elemental sulphur, as suggested in Figures 3 and 10; and (3), there may be differences in sample packing that affect access to oxygen and moisture.

These possibilities help explain the finding that the same samples can vary in response to the degree of weathering (Figure 11). This variation is mirrored in the field where self-heating typically occurs in isolated “hot spots” and not generally across the entire pile [18].

The standard Stage A/Stage B test tends not to encounter variations in response on the same sample. In these tests the temperature in Stage B is set at 140 °C consequently whether transition occurs is not at issue. The test, designed to identify a material’s propensity to self-heat and progress from Stage A to Stage B (and by extension Stage C), is independent of whether, on occasions, conditions may suppress transition. Testing in adiabatic mode, as introduced here, does offer further insights into the self-heating process and complements the standard FR-2 test.

6. Conclusions

This study focused on the transition from Stage A to Stage B in the self-heating of sulphides. A new test using adiabatic conditions is introduced. Evidence is presented that the transition occurs at 96 °C, corresponding to the transition from the stable rhombic form of elemental sulphur to the more reactive monoclinic form. The transition temperature, formerly designated as 100 °C, is duly revised to 96 °C. Variations in sample response to transitioning are detected and possible reasons are discussed.

Author Contributions: Conceptualization: J.A.F., F.R. and S.M.; methodology: J.A.F., F.R. and S.M.; validation: J.A.F., F.R. and S.M.; formal analysis: J.A.F., F.R. and S.M.; investigation: S.M.; data curation: J.A.F. and F.R.; writing—original draft preparation: S.M. and Y.T.; writing—review and editing: J.A.F., F.R., K.E.W. and Y.T.; visualization: Y.T. and F.R.; supervision: J.A.F. and K.E.W.; project administration: J.A.F. and K.E.W.; funding acquisition: J.A.F. and K.E.W. All authors have read and agreed to the published version of the manuscript.

Funding: The work was conducted under the Chair in Mineral Processing funded through the NSERC (Natural Sciences and Engineering Research Council of Canada, NSERC CRDPJ 445682-12) CRD (Collaborative Research and Development) program sponsored by Vale, Teck, Xstrata Process Support, Barrick Gold, Shell Canada, Corem, SGS Lakefield Research and Flottec. Provision of the test samples and discussions with Glencore personnel are gratefully acknowledged.

Conflicts of Interest: The authors declare no conflict of interest. The funders had no role in the design of the study; in the collection, analyses, or interpretation of data; in the writing of the manuscript, or in the decision to publish the result.

References

1. Beever, P.F.; Crowhurst, D. Fire and explosion hazards associated with milk spray drying operations. *Int. J. Dairy Technol.* **1989**, *42*, 65–70. [[CrossRef](#)]
2. Hudak, P.F. Spontaneous combustion of shale spoils at a sanitary landfill. *Waste Manag.* **2002**, *22*, 687–688. [[CrossRef](#)]
3. Rosenblum, F.; Nessel, J.; Spira, P. Evaluation and control of self-heating in sulphide concentrates. *CIM Bull.* **2001**, *94*, 92–99.
4. Payant, R.; Rosenblum, F.; Nessel, J.E.; Finch, J.A. The self-heating of sulfides: Galvanic effects. *Miner. Eng.* **2012**, *26*, 57–63. [[CrossRef](#)]
5. Ninteman, D.J. *Spontaneous Oxidation and Combustion of Sulfide Ores in Underground Mines: A Literature Survey*; US Government Printing Office, Department of the Interior, Bureau of Mines: Washington, DC, USA, 1978; Volume 8775.
6. Farnsworth, D.J.; Duties, S. Introduction to and background of sulphide fires in pillar mining at the Sullivan Mine. *CIM Bull.* **1977**, *70*, 65–71.
7. Kirshenbaum, N.W. *Transport and Handling of Sulphide Concentrates: Problems and Possible Improvements*; Technomic Pub. Co.: Stanford, CA, USA, 1968.
8. Anon. Amendments (05–19) to the International Maritime Solid Bulk Cargoes Code, Lloyd’s Register, Class News 21/2019. Available online: <https://info.lr.org/l/12702/2019--11-18/86y6tv> (accessed on 3 December 2020).
9. Rosenblum, F.; Spira, P. Evaluation of hazard from self-heating of sulphide rock. *CIM Bull.* **1995**, *88*, 44–49.
10. Wu, C.; Li, Z. A simple method for predicting the spontaneous combustion potential of sulphide ores at ambient temperature (Technical note). *Min. Technol. Trans. Inst. Min. Metall. Sect. A* **2005**, *114*, 125–128.
11. Bouffard, S.C.; Senior, G.D. A new method for testing the self-heating character of sulphide concentrates. *Miner. Eng.* **2011**, *24*, 1517–1519. [[CrossRef](#)]
12. Dai, Z. Development of an experimental methodology for sulphide self-heating studies and the self-heating tendency of Vale’s Voisey’s Bay Concentrator products. *Miner. Eng.* **2016**, *92*, 125–133. [[CrossRef](#)]
13. Moon, S.; Frank, R.; Tan, Y.H.; Nessel, J.E.; Waters, K.E.; Finch, J.A. Examination of the United Nations self-heating test for sulphides. *Can. Metall. Q.* **2019**, *58*, 438–444. [[CrossRef](#)]
14. Habashi, F. The mechanism of oxidation of sulfide ores in nature. *Econ. Geol.* **1966**, *61*, 587–591. [[CrossRef](#)]
15. Tributsch, H.; Gerischer, H. The oxidation and self-heating of metal sulphides as an electrochemical corrosion phenomenon. *J. Appl. Chem. Biotechnol.* **1976**, *26*, 747–761. [[CrossRef](#)]
16. Rosenblum, F.; Spira, P. Self-heating of sulphides. In Proceedings of the 13th Annual Meeting of the Canadian Minerals Processors, CIM, Ottawa, ON, Canada, 20–21 January 1981; Paper 3. pp. 34–51.
17. Rosenblum, F.; Spira, P.; Konigsmann, K.V. Evaluation of hazard from backfill oxidation. *CIM Bull.* **1982**, *75*, 87–98.
18. Rosenblum, F.; Spira, P. Evaluation of hazard from sulphide rock oxidation, In Proceedings of the 11th Underground Operators Conference, CIM, Saskatoon, SK, Canada, 21–24 February 1993.
19. Payant, R.; Rosenblum, F.; Nessel, J.E.; Finch, J.A. Galvanic interaction and particle size effects in self-heating of sulphide mixtures. In *Separation Technologies for Minerals, Coal, and Earth Resources*; Young, C., Luttrell, G.H., Eds.; Society for Mining, Metallurgy, and Exploration (SME): Englewood, CO, USA, 2012; pp. 419–429.
20. Rosenblum, F.; Finch, J.A.; Waters, K.E.; Nessel, J.E. A test apparatus for studying the effects weathering on self-heating of sulphides. In Proceedings of the Conference of Metallurgists (COM), Montreal, QC, Canada, 23–26 August 2015; pp. 1–12.
21. Loomis, I.M.; Hughes, S.; Osborne, K.; Basyuni, J.; Samosir, E. Control of a sulfide ore thermal event in a drawpoint at PT Freeport Indonesia’s DOZ Mine, Papua, Indonesia. In Proceedings of the 12th U.S./North American Mine Ventilation Symposium, Reno, NV, USA, 9–11 June 2008; Wallace, K.G., Ed.; University of Nevada Press: Reno, NV, USA, 2008; pp. 533–538.
22. Meyer, B. Elemental sulfur. *Chem. Rev.* **1976**, *76*, 367–388. [[CrossRef](#)]
23. Bojes, J.; Lerbscher, J.; Wamburi, W.; Dille, C. Elemental Sulphur in 3-phase sour gas systems—Is condensate really your ally? In Proceedings of the Norther Area Western Conference, Calgary, AB, Canada, 15–18 February 2010; pp. 1–22.
24. Turova, N. Sulphur. In *Inorganic Chemistry in Tables*; Springer: New York, NY, USA; Berlin/Heidelberg, Germany, 2011.

25. Griebel, J.J.; Glass, R.S.; Char, K.; Pyun, J. Polymerizations with elemental sulfur: A novel route to high sulfur content polymers for sustainability, energy and defense. *Prog. Polym. Sci.* **2016**, *58*, 90–125. [[CrossRef](#)]
26. Davis, C.S.; Hyne, J.B. Thermomechanical analysis of elemental sulphur: The effects of thermal history and ageing. *Thermochim. Acta* **1976**, *15*, 375–385. [[CrossRef](#)]
27. Rosenblum, F.; Finch, J.A.; Nessel, J. The key role of sample weathering in self-heating testing methodologies for sulphides. In Proceedings of the XXVII International Mineral Processing Congress (IMPC), Santiago, Chile, 20–24 October 2014; pp. 111–123.
28. Steger, H.F. Determination of the elemental sulphur content of minerals and ores. *Talanta* **1976**, *23*, 395–397. [[CrossRef](#)]

Publisher's Note: MDPI stays neutral with regard to jurisdictional claims in published maps and institutional affiliations.



© 2020 by the authors. Licensee MDPI, Basel, Switzerland. This article is an open access article distributed under the terms and conditions of the Creative Commons Attribution (CC BY) license (<http://creativecommons.org/licenses/by/4.0/>).